Electron self-energy effects on chiral symmetry breaking in graphene

J. González

Instituto de Estructura de la Materia, Consejo Superior de Investigaciones Científicas, Serrano 123, 28006 Madrid, Spain

(Dated: February 3, 2012)

We investigate the dynamical breakdown of the chiral symmetry in the theory of Dirac fermions in graphene with long-range Coulomb interaction. We analyze the electron-hole vertex relevant for the dynamical gap generation in the ladder approximation, showing that it blows up at a critical value α_c in the graphene fine structure constant which is quite sensitive to many-body corrections. Under static RPA screening of the interaction potential, we find that taking into account electron self-energy corrections to the vertex increases the critical coupling to $\alpha_c \approx 4.9$, for a number $N = 4$ of two-component Dirac fermions. When dynamical screening of the interaction is instead considered, the effect of Fermi velocity renormalization in the electron and hole states leads to the value $\alpha_c \approx 1.75$ for $N = 4$, substantially larger than that obtained without electron self-energy corrections (≈ 0.99), but still below the nominal value of the interaction coupling in isolated free-standing graphene.

I. INTRODUCTION

The discovery of graphene, the material made of a one-atom-thick carbon layer, has attracted a lot attention as it provides the realization of a system where the electrons have conical valence and conduction bands, therefore behaving at low energies as massless Dirac fermions[1–3]. This offers the possibility of employing the new material as a test ground of fundamental concepts in theoretical physics, since the interacting electron system represents a variant of strongly coupled quantum electrodynamics (QED) affording quite unusual effects[4–7].

A remarkable feature of such a theory is that a sufficiently strong Coulomb interaction may open a gap in the electronic spectrum. This effect was already known from the study of QED [8], where it corresponds to the dynamical breakdown of the chiral $U(2)$ symmetry of the theory. In the context of graphene, such a mechanism is sometimes alluded as an exciton instability though, given the absence of a gap between valence and conduction bands, it becomes more appropriate to describe the effect as a kind of charge-density-wave instability of the 2D layer. The gap generation proceeds actually through the development of a non-vanishing average value of the staggered (sublattice odd) charge density in the underlying honeycomb lattice, which leads to the generation of a mass and opening of a gap for the Dirac quasiparticles.

The question of the dynamical gap generation was first addressed in graphene in the approach to the theory with a large number N of fermion flavors[9–12]. The existence of a critical point for the formation of an excitonic insulator has been also suggested from second-order calculations of electron self-energy corrections[13]. More recently, Monte Carlo simulations of the field theory have been carried out in the graphene lattice[14, 15], showing that the chiral symmetry of the massless theory can be broken above a critical value for the graphene fine structure constant $\alpha_c \approx 1.08$ [14]. The possibility of dynamical gap generation has been also studied in the ladder approximation[16–19], leading in the case of static screening of the interaction to an estimate of the critical coupling $\alpha_c \approx 1.62$ for $N = 4$ [16]. Lately, the resolution of the Schwinger-Dyson formulation of the gap equation has revealed that the effect of the dynamical polarization can significantly lower the critical coupling for dynamical gap generation, down to a value $\alpha_c \approx 0.92$ for $N = 4$[20].

In this paper we take advantage of the renormalization properties of the Dirac theory in order to assess the effect of the electron self-energy corrections on the chiral symmetry breaking. In this respect, it has been found that the renormalization of the quasiparticle properties can have a significant impact, mainly through the increase of the Fermi velocity at low energies[21, 22]. Then, we will consider the electron-hole vertex accounting for the dynamical gap generation in the ladder approximation, shown schematically in Fig. 1, and we will supplement it by self-energy corrections to the electron and hole states. This dressing of the quasiparticles will have the result of increasing significantly the critical coupling at which the chiral symmetry breaking takes place. Thus, under static RPA screening of the interaction potential in the ladder series, we will find the critical value $\alpha_c \approx 4.9$ at the physical number of flavors $N = 4$. In agreement with the trend observed in Ref. [20], we will see however that the more sensible dynamical screening of the interaction has the effect of lowering substantially that estimate, down to a value $\alpha_c \approx 1.75$ which is below the nominal value of the interaction coupling in isolated free-standing graphene.

II. LADDER APPROXIMATION FOR STAGGERED CHARGE DENSITY

We consider the field theory for Dirac quasiparticles in graphene interacting through the long-range Coulomb potential, with a Hamiltonian given by

$$H = i v_F \int d^2 r \; \overline{\psi}_i(\mathbf{r}) \boldsymbol{\gamma} \cdot \boldsymbol{\nabla} \psi_i(\mathbf{r})$$
$$+ \frac{e^2}{8\pi} \int d^2 r_1 \int d^2 r_2 \; \rho(\mathbf{r}_1) \frac{1}{|\mathbf{r}_1 - \mathbf{r}_2|} \rho(\mathbf{r}_2) \qquad (1)$$

where $\{\psi_i\}$ is a collection of $N/2$ four-component Dirac spinors, $\overline{\psi}_i = \psi_i^\dagger \gamma_0$, and $\rho(\mathbf{r}) = \overline{\psi}_i(\mathbf{r})\gamma_0\psi_i(\mathbf{r})$. The matrices γ_σ satisfy $\{\gamma_\mu, \gamma_\nu\} = 2\,\mathrm{diag}(1, -1, -1)$ and can be

conveniently represented in terms of Pauli matrices as $\gamma_{0,1,2} = (\sigma_3, \sigma_3\sigma_1, \sigma_3\sigma_2) \otimes \sigma_3$, where the first factor acts on the two sublattice components of the graphene lattice.

Our main interest is to study the behavior of the vertex for the staggered (sublattice odd) charge density

$$\rho_m(\mathbf{r}) = \overline{\psi}(\mathbf{r})\psi(\mathbf{r}) \qquad (2)$$

This operator gives the order parameter for the dynamical gap generation, and the signal that it gets a nonvanishing expectation value can be obtained from the divergence of the response function $\langle T\rho_m(\mathbf{q},t)\rho_m(-\mathbf{q},0)\rangle$. The singular behavior of this susceptibility can be traced back to the divergence at $\mathbf{q}, \omega_q \to 0$ of the irreducible vertex

$$\Gamma(\mathbf{q},\omega_q;\mathbf{k},\omega_k)$$
$$= \langle \rho_m(\mathbf{q},\omega_q)\psi(\mathbf{k}+\mathbf{q},\omega_k+\omega_q)\psi^\dagger(\mathbf{k},\omega_k)\rangle_{1\mathrm{PI}} \quad (3)$$

where 1PI denotes that Γ is made of one-particle irreducible diagrams without external electron propagators.

In the ladder approximation, the vertex Γ is bound to satisfy the self-consistent equation depicted diagrammatically in Fig. 1. This equation can be solved perturbatively by iterating the interaction between electrons and holes in the vertex, in which case this ends up being represented by the sum of ladder diagrams. On the other hand, the self-consistent equation can be written in compact form, specially at momentum transfer $\mathbf{q} = 0$ and $\omega_q = 0$. We recall at this point the expression of the free Dirac propagator

$$\langle \psi(\mathbf{k},\omega_k)\psi^\dagger(\mathbf{k},\omega_k)\rangle_{\mathrm{free}} = i\frac{-\gamma_0\omega_k + v_F\boldsymbol{\gamma}\cdot\mathbf{k}}{-\omega_k^2 + v_F^2\mathbf{k}^2 - i\eta}\gamma_0 \qquad (4)$$

Given that Γ must be anyhow proportional to γ_0, we get

$$-\frac{-\gamma_0\omega_p + v_F\boldsymbol{\gamma}\cdot\mathbf{p}}{-\omega_p^2 + v_F^2\mathbf{p}^2 - i\eta}\gamma_0\, \Gamma(\mathbf{0},0;\mathbf{p},\omega_p)\, \frac{-\gamma_0\omega_p + v_F\boldsymbol{\gamma}\cdot\mathbf{p}}{-\omega_p^2 + v_F^2\mathbf{p}^2 - i\eta}\gamma_0$$
$$= \frac{\Gamma(\mathbf{0},0;\mathbf{p},\omega_p)}{-\omega_p^2 + v_F^2\mathbf{p}^2 - i\eta} \qquad (5)$$

The self-consistent equation for the vertex becomes then

$$\Gamma(\mathbf{0},0;\mathbf{k},i\omega_k) = \gamma_0$$
$$+ \int \frac{d^2p}{(2\pi)^2}\frac{d\omega_p}{2\pi}\frac{\Gamma(\mathbf{0},0;\mathbf{p},i\omega_p)}{\omega_p^2 + v_F^2\mathbf{p}^2}V(\mathbf{k}-\mathbf{p},i\omega_k-i\omega_p) \quad (6)$$

where $V(\mathbf{p},\omega_p)$ stands for the Coulomb interaction. We will deal in general with the RPA to screen the potential, so that

$$V(\mathbf{p},\omega_p) = \frac{e^2}{2|\mathbf{p}| + e^2\chi(\mathbf{p},\omega_p)} \qquad (7)$$

in terms of the polarization χ for N two-component Dirac fermions.

Eq. (6) is formally invariant under a dilatation of frequencies and momenta, which shows that the scale

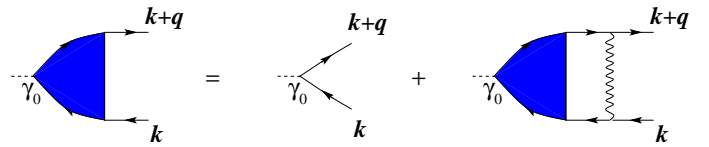FIG. 1: Self-consistent diagrammatic equation for the vertex $\langle \rho_m(\mathbf{q},\omega_q)\psi(\mathbf{k}+\mathbf{q},\omega_k+\omega_q)\psi^\dagger(\mathbf{k},\omega_k)\rangle$, equivalent to the sum of ladder diagrams built from the iteration of the Coulomb interaction (wavy line) between electron and hole states (arrow lines).

of $\Gamma(\mathbf{0},0;\mathbf{k},\omega_k)$ is dictated by the high-energy cutoff Λ needed to regularize the integrals. The vertex acquires in general an anomalous dimension γ_{ψ^2}, which governs the behavior under changes in the energy scale[23]

$$\Gamma(\mathbf{q},\omega_q;\mathbf{k},\omega_k) \sim \Lambda^{\gamma_{\psi^2}} \qquad (8)$$

We recall below how to compute γ_{ψ^2}, showing that it diverges at a critical value of the interaction strength $\alpha = e^2/4\pi v_F$. This translates into a divergence of the own susceptibility $\langle T\rho_m(\mathbf{q},t)\rho_m(-\mathbf{q},0)\rangle$ at momentum transfer $\mathbf{q} \to 0$, providing then the signature of the condensation of $\rho_m(\mathbf{r}) = \overline{\psi}(\mathbf{r})\psi(\mathbf{r})$ and the consequent development of the gap for the Dirac quasiparticles.

III. ELECTRON SELF-ENERGY EFFECTS IN STATICALLY SCREENED LADDER APPROXIMATION

We deal first with the approach in which electrons and holes are dressed by self-energy corrections, while the Coulomb interaction in (6) is screened by means of the static RPA with polarization

$$\chi(\mathbf{p},0) = \frac{N}{16}\frac{|\mathbf{p}|}{v_F} \qquad (9)$$

The most important self-energy effect comes from the renormalization of the Fermi velocity at low energies[24, 25], which can be incorporated by replacing v_F in Eq. (6) by the effective Fermi velocity

$$\widetilde{v}_F(\mathbf{p}) = v_F + \Sigma_v(\mathbf{p}) \qquad (10)$$

dressed with the self-energy corrections $\Sigma_v(\mathbf{p})$. The expansion of Eq. (6) in powers of $\Sigma_v(\mathbf{p})$ would amount to the iteration of self-energy corrections in the electron and hole internal lines in Fig. 1, showing that the present approach encodes a systematic way of improving the sum of ladder diagrams for the vertex Γ [26].

The electron self-energy corrections, as well as the terms of the ladder series, are given by logarithmically divergent integrals that need to be cut off at a high-energy scale Λ. Alternatively, one can also define the theory at spatial dimension $D = 2 - \epsilon$, what automatically regularizes all the momentum integrals. After performing the
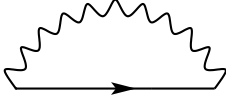
FIG. 2: Electron self-energy correction leading to a divergent renormalization of the Fermi velocity v_F.

frequency integral, Eq. (6) then becomes

$$\Gamma(\mathbf{0},0;\mathbf{k},\omega_k) = \gamma_0$$
$$+ \frac{e_0^2}{4\kappa} \int \frac{d^D p}{(2\pi)^D} \Gamma(\mathbf{0},0;\mathbf{p},\omega_k) \frac{1}{\widetilde{v}_F(\mathbf{p})|\mathbf{p}|} \frac{1}{|\mathbf{k}-\mathbf{p}|} \quad (11)$$

where e_0^2 is related to e^2 through an auxiliary momentum scale ρ such that

$$e_0^2 = \rho^\epsilon e^2 \quad (12)$$

and we have defined the dielectric constant

$$\kappa = 1 + \frac{N e^2}{32 v_F} \quad (13)$$

In the ladder approximation, the Fermi velocity gets a divergent correction only from the "rainbow" self-energy diagram with exchange of a single screened interaction shown in Fig. 2 [24]. The dressed Fermi velocity becomes

$$\widetilde{v}_F(\mathbf{p}) = v_F + \frac{e_0^2}{16\pi^2\kappa} (4\pi)^{\epsilon/2} \frac{\Gamma(\frac{\epsilon}{2})\Gamma(\frac{1-\epsilon}{2})\Gamma(\frac{3-\epsilon}{2})}{\Gamma(2-\epsilon)} \frac{1}{|\mathbf{p}|^\epsilon} \quad (14)$$

The expressions (11) and (14) are singular in the limit $\epsilon \to 0$. The most convenient way to show that all the poles in the ϵ parameter can be renormalized away is to resort at this point to a perturbative computation of $\Gamma(\mathbf{0},0;\mathbf{k},\omega_k)$.

The solution of (11) can be obtained in the form

$$\Gamma(\mathbf{0},0;\mathbf{k},\omega_k) = \gamma_0 \left(1 + \sum_{n=1}^{\infty} \lambda_0^n \frac{r_n}{|\mathbf{k}|^{n\epsilon}} \right) \quad (15)$$

with $\lambda_0 = e_0^2/4\pi\kappa v_F$. Each term in the sum can be obtained from the previous one by expanding $1/\widetilde{v}_F(\mathbf{p})$ in Eq. (11) in powers of e_0^2 and noticing that

$$\int \frac{d^D p}{(2\pi)^D} \frac{1}{|\mathbf{p}|^{(m-1)\epsilon}} \frac{1}{|\mathbf{p}|} \frac{1}{|\mathbf{k}-\mathbf{p}|}$$
$$= \frac{(4\pi)^{\epsilon/2}}{4\pi^{3/2}} \frac{\Gamma\left(\frac{m\epsilon}{2}\right)\Gamma\left(\frac{1-m\epsilon}{2}\right)\Gamma\left(\frac{1-\epsilon}{2}\right)}{\Gamma\left(\frac{1+(m-1)\epsilon}{2}\right)\Gamma\left(1-\frac{m+1}{2}\epsilon\right)} \frac{1}{|\mathbf{k}|^{m\epsilon}} \quad (16)$$

At each given perturbative level, the vertex displays then a number of poles at $\epsilon = 0$. The crucial point is that these divergences can be reabsorbed by passing to physical quantities defined by the multiplicative renormalization

$$v_F = Z_v (v_F)_{\text{ren}} \quad (17)$$
$$\overline{\psi}\psi = Z_{\psi^2} (\overline{\psi}\psi)_{\text{ren}} \quad (18)$$

We observe that the scale of the single Dirac field ψ does not need to be renormalized in this approach, as self-energy corrections of the form shown in Fig. 2 with a statically screened interaction do not modify the frequency dependence of the Dirac propagator.

The renormalized vertex

$$\Gamma_{\text{ren}} = Z_{\psi^2} \Gamma \quad (19)$$

can be actually made finite at $\epsilon = 0$ with a suitable choice of momentum-independent factors Z_v and Z_{ψ^2}. Z_v must be chosen to cancel the $1/\epsilon$ pole arising from $\Gamma(\epsilon/2)$ in (14), and it has therefore the simple structure

$$Z_v = 1 + \frac{b_1}{\epsilon} \quad (20)$$

with $b_1 = -e^2/16\pi\kappa(v_F)_{\text{ren}}$. On the other hand, we have the general structure

$$Z_{\psi^2} = 1 + \sum_{i=1}^{\infty} \frac{c_i}{\epsilon^i} \quad (21)$$

The position of the different poles must be chosen to enforce the finiteness of $\Gamma_{\text{ren}} = Z_{\psi^2} \Gamma$ in the limit $\epsilon \to 0$. The computation of the first orders of the expansion gives for instance the result

$$c_1(\lambda) = -\frac{1}{2}\lambda - \frac{1}{8}\log(2)\,\lambda^2 - \frac{1}{1152}\left(\pi^2 + 120\log^2(2)\right)\lambda^3$$
$$- \frac{10\pi^2\log(2) + 688\log^3(2) + 15\zeta(3)}{6144}\lambda^4$$
$$- \frac{13\pi^4 + 2064\pi^2\log^2(2) + 144\left(716\log^4(2) + 37\log(2)\zeta(3)\right)}{737280}\lambda^5$$
$$+ \cdots$$
$$c_2(\lambda) = \frac{1}{16}\lambda^2 + \frac{1}{24}\log(2)\,\lambda^3$$
$$+ \frac{1}{18432}\left(5\pi^2 + 744\log^2(2)\right)\lambda^4$$
$$+ \frac{110\pi^2\log(2) + 8592\log^3(2) + 135\zeta(3)}{184320}\lambda^5 + \cdots$$
$$c_3(\lambda) = -\frac{1}{768}\log(2)\,\lambda^4 - \frac{1}{184320}\left(\pi^2 + 360\log^2(2)\right)\lambda^5$$
$$+ \cdots$$
$$c_4(\lambda) = -\frac{1}{7680}\log(2)\,\lambda^5 + \cdots \quad (22)$$

where the series are written in terms of the renormalized coupling λ defined by

$$\lambda \equiv \rho^{-\epsilon} Z_v \lambda_0 = \frac{e^2}{4\pi\kappa(v_F)_{\text{ren}}} \quad (23)$$

The physical observable in which we are interested is the anomalous dimension γ_{ψ^2}. The change in the dimension of Γ_{ren} comes from the dependence of Z_{ψ^2} on the only dimensionful scale ρ in the renormalized theory. Therefore we have[23]

$$\gamma_{\psi^2} = \frac{\rho}{Z_{\psi^2}} \frac{\partial Z_{\psi^2}}{\partial \rho} \quad (24)$$

The original bare theory at $D \neq 2$ does not know about the arbitrary scale ρ, and the independence of
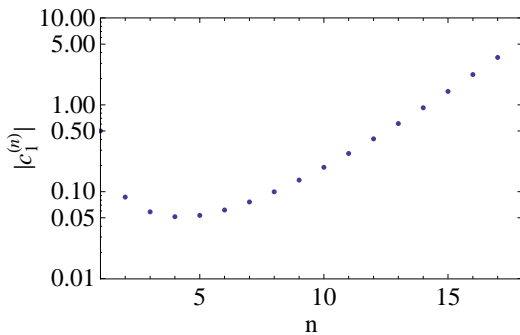
FIG. 3: Plot of the absolute value of the coefficients $c_1^{(n)}$ in the expansion of $c_1(\lambda)$ as a power series of the coupling λ.

$\lambda_0 = \rho^\epsilon \lambda / Z_v$ on that variable leads to

$$\rho \frac{\partial \lambda}{\partial \rho} = -\epsilon \lambda - \lambda b_1(\lambda) \qquad (25)$$

At $\epsilon = 0$, this is the well-known expression of the scale dependence of the effective interaction strength, arising from the renormalization of the Fermi velocity[24]. The anomalous dimension becomes finally[27]

$$\gamma_{\psi^2} = \frac{\rho}{Z_{\psi^2}} \frac{\partial \lambda}{\partial \rho} \frac{\partial Z_{\psi^2}}{\partial \lambda} = -\lambda \frac{dc_1}{d\lambda} \qquad (26)$$

In the derivation of (26), it is implicitly assumed that poles in the ϵ parameter cannot appear at the right-hand-side of the equation. For this to be true, the set of equations

$$\frac{dc_{i+1}}{d\lambda} = c_i \frac{dc_1}{d\lambda} - b_1 \frac{dc_i}{d\lambda} \qquad (27)$$

must be satisfied identically[27]. Quite remarkably, we have verified that this is the case, up to the order λ^{17} we have been able to compute numerically the coefficients in (21). This is the proof of the renormalizability of the theory, which guarantees that physical quantities like γ_{ψ^2} remain finite in the limit $\epsilon \to 0$.

From the practical point of view, the important result is the evidence that the perturbative expansion of $c_1(\lambda)$

$$c_1(\lambda) = \sum_n c_1^{(n)} \lambda^n \qquad (28)$$

approaches a geometric series in the λ variable. The plot of the coefficients $c_1^{(n)}$ computed numerically up to order λ^{17} is shown in Fig. 3. It can be checked that the coefficients grow exponentially with the order n, in such a way that

$$-c_1(\lambda) \geq \sum_{n=1}^{\infty} d^n \lambda^n + \text{regular terms} \qquad (29)$$

An estimate of d can be obtained from the coefficients available in the perturbative series of $c_1(\lambda)$. The ratio
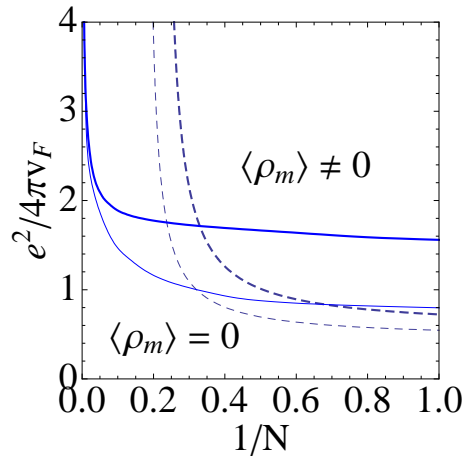

FIG. 4: Phase diagram showing the boundary between the metallic phase and the phase with dynamical gap generation ($\langle \rho_m \rangle \neq 0$) in the ladder approximation. The thin dashed (solid) line represents the phase boundary obtained with static (dynamic) RPA screening of the interaction potential and no electron self-energy corrections. The thick dashed (solid) line represents the boundary after including the effect of the electron self-energy corrections on top of the static (dynamic) RPA screening of the interaction in the ladder series.

between consecutive $c_1^{(n)}$ increases with the order n, converging towards a limit value. The best fit of the asymptotic behavior allows us to estimate a radius of convergence

$$\lambda_c \approx 0.56 \qquad (30)$$

This has to be compared with the value found in the approach neglecting self-energy corrections, which leads to $\lambda_c \approx 0.45$ [18], in close agreement with the result of Ref. 16. The critical coupling in the variable λ can be used to draw the boundary for dynamical gap generation in the space of N and $\alpha = e^2/4\pi(v_F)_{\text{ren}}$, recalling that

$$\lambda = \frac{\alpha}{1 + \frac{N\pi}{8}\alpha} \qquad (31)$$

The corresponding phase diagram is represented in Fig. 4. For $N = 4$, we get in particular the critical coupling $\alpha_c \approx 4.9$, significantly above the critical value that would be obtained from the radius of convergence without self-energy corrections ($\alpha_c \approx 1.53$).

IV. ELECTRON SELF-ENERGY EFFECTS IN DYNAMICALLY SCREENED LADDER APPROXIMATION

In the framework of the ladder approximation, one can also study the effect of electron self-energy corrections under dynamical screening of the Coulomb interaction potential. We can improve the static RPA by considering

the full effect of the frequency-dependent polarization, which for Dirac fermions takes the form[24]

$$\chi(\mathbf{p}, \omega_p) = \frac{N}{16} \frac{\mathbf{p}^2}{\sqrt{v_F^2 \mathbf{p}^2 - \omega_p^2}} \qquad (32)$$

This expression can be introduced in Eq. (6) to look again for self-consistent solutions for the vertex $\Gamma(\mathbf{0}, 0; \mathbf{k}, \omega_k)$. Given that in this case we must resort to numerical methods for the resolution of the integral equation, we can go beyond the self-energy effects considered before by taking into account the electron self-energy corrections in the RPA improved with the polarization (32). In this approach, the behavior of the dressed Fermi velocity $\widetilde{v}_F(\mathbf{p})$ is given as a function of $g = Ne^2/32\widetilde{v}_F$ by the nonlinear equation[25]

$$\frac{\partial \log \widetilde{v}_F}{\partial \log |\mathbf{p}|} = -\frac{8}{N\pi^2}\left(1 + \frac{\arccos g}{g\sqrt{1-g^2}} - \frac{\pi}{2}\frac{1}{g}\right) \qquad (33)$$

We have then used the solution of Eq. (33) to replace v_F in Eq. (6) by the momentum dependent $\widetilde{v}_F$, which represents a significant improvement in the sum of self-energy corrections in the ladder series for the vertex.

In this procedure, we find again that there is a critical coupling in the variable $\alpha = e^2/4\pi v_F$ at which $\Gamma(\mathbf{0}, 0; \mathbf{k}, \omega_k)$ blows up, marking the boundary between two different regimes where Eq. (6) has respectively positive and negative solutions. In practice, we have solved the integral equation by defining the vertex in a discrete set of points in frequency and momentum space. One can take as independent variables in $\Gamma(\mathbf{0}, 0; \mathbf{k}, \omega_k)$ the modulus of $\mathbf{k}$ and positive frequencies ω_k. We have adopted accordingly a grid of dimension $l \times l$ covering those variables, with l running up to a value of 200 for which it is still viable to invert a matrix of dimension l^2.

As a check of our approach, we have compared the results of the numerical diagonalization of (6), still keeping the undressed Fermi velocity v_F, with the values of the critical coupling in Ref. [20], where the resolution of the gap equation has been accomplished with the frequency-dependent polarization. We have relied on the scale invariance of our model to find the trend of α_c at large l, as the critical coupling must obey a finite-size scaling law

$$\alpha_c(l) = \alpha_c(\infty) + \frac{c}{l^\nu} \qquad (34)$$

At $N = 4$, we get $\alpha_c(200) \approx 1.08$ and the estimate $\alpha_c(\infty) \approx 0.99$, which turns out to be close to the critical coupling $\alpha_c \approx 0.92$ found in Ref. [20], providing a nice check of our computational approach in the case of unrenormalized v_F.

The electron self-energy corrections lead anyhow to a substantial increase in the values of the critical coupling $\alpha_c(l)$. This is a decreasing function of l, as the limit $l \to \infty$ corresponds to the large-volume limit of the system. Then, as a result of diagonalizing Eq. (6) with the

effective $\widetilde{v}_F$, we have chosen to represent in Fig. 4 the upper bound $\alpha_c(200)$ to the critical coupling as a function of N. We observe that, for $N \lesssim 3$, the values of the critical coupling are larger than those obtained with static screening of the interaction potential, while the situation is inverted for $N \gtrsim 3$. In coincidence with the findings of Ref. [20], there is indeed no upper limit on N for the onset of chiral symmetry breaking in this approach. At $N = 4$, we get

$$\alpha_c(200) \approx 1.75 \qquad (35)$$

which is substantially smaller than the value found in Sec. III with the static RPA screening in the ladder series. These results support the idea that, in the particular case of graphene ($N = 4$), the nominal coupling of the system in vacuum ($\alpha \approx 2.2$) should be above the critical coupling for dynamical gap generation. This is reinforced by the fact that other effects neglected thus far have to do with the electron self-energy corrections to the own polarization χ. These should lead to a reduction of the screening and the consequent enhancement of the effective interaction strength. The values that we find for α_c should be taken in this regard as an upper bound for the critical coupling, at least when compared with the result of including the effect of Fermi velocity renormalization in the bare polarization.

V. CONCLUSION

In this paper we have considered the impact that electron self-energy corrections may have on the chiral symmetry breaking in the interacting theory of Dirac fermions. Our starting point has been the ladder approximation for the electron-hole vertex appearing in the response function for dynamical gap generation, which we have supplemented by including systematically the self-energy corrections to electron and hole states in the ladder series.

In this framework, we have been able to account for the effect of the Fermi velocity renormalization on the critical coupling for dynamical gap generation. In this respect, it has been already suggested that the growth of the Fermi velocity at low energies can have a deep impact to prevent the chiral symmetry breaking[22, 28]. The scale dependence of the Fermi velocity, expressed nonperturbatively in Eq. (33), has been already observed in experiments with graphene at very low doping levels[29]. Our results show actually that the effect of renormalization of the Fermi velocity induces a significant reduction in the strength of the dynamical symmetry breaking in graphene, leading to a critical coupling $\alpha_c \approx 4.9$ in the case of static RPA screening of the interaction potential in the ladder series, and to a value $\alpha_c \approx 1.75$ in the more sensible instance of dynamical screening of the interaction.

One of the main conclusions of this work is that the screening effects must be treated accurately in order to

make a reliable estimate of the critical coupling for dynamical gap generation in graphene. This is so as such an instability depends strongly on the singular behavior of the Coulomb interaction in the undoped system. In this regard, the situation is quite different to the case of bilayer graphene, where several low-energy instabilities have been also predicted[30–33]. These can be traced back to the divergence of objects like the electron-hole polarization, which results from the particular form of the bandstructure and does not require a long-range interaction. In monolayer graphene, the instability towards chiral symmetry breaking appears to be quite sensitive to many-body corrections to the Coulomb interaction, which makes more delicate the precise computation of the critical interaction strength.

The other important conclusion is that the value $\alpha_c \approx 1.75$ resulting from the self-energy corrections still remains below the nominal coupling for graphene in vacuum. This means that an isolated free-standing layer of the material should be in the phase with dynamical gap generation, which is apparently at odds with present experimental measurements in suspended graphene samples. A key observation is however that, if chiral symmetry breaking is to proceed in graphene according to the present estimates, it is going to lead to a gap at least three orders of magnitude below the high-energy scale of the Dirac theory, as found in the resolution of the gap equation[20]. This suggests then that the dynamical gap generation cannot be discarded in isolated free-standing graphene, though its experimental signature may be only found in suitable samples, for which the Fermi level can be tuned within an energy range below the meV scale about the charge neutrality point.

[1] K. S. Novoselov, A. K. Geim, S. V. Morozov, D. Jiang, M. I. Katsnelson, I. V. Grigorieva, S. V. Dubonos and A. A. Firsov, Nature **438**, 197 (2005).
[2] Y. Zhang, Y.-W. Tan, H. L. Stormer and P. Kim, Nature **438**, 201 (2005).
[3] A. H. Castro Neto, F. Guinea, N. M. R. Peres, K. S. Novoselov and A. K. Geim, Rev. Mod. Phys. **81**, 109 (2009).
[4] V. M. Pereira, J. Nilsson and A. H. Castro Neto, Phys. Rev. Lett. **99**, 166802 (2007).
[5] M. M. Fogler, D. S. Novikov, and B. I. Shklovskii, Phys. Rev. B **76**, 233402 (2007).
[6] A. V. Shytov, M. I. Katsnelson, and L. S. Levitov, Phys. Rev. Lett. **99**, 236801 (2007).
[7] I. S. Terekhov, A. I. Milstein, V. N. Kotov, and O. P. Sushkov, Phys. Rev. Lett. **100**, 076803 (2008).
[8] T. Appelquist, D. Nash and L. C. R. Wijewardhana, Phys. Rev. Lett. **60**, 2575 (1988).
[9] D. V. Khveshchenko, Phys. Rev. Lett. **87**, 246802 (2001).
[10] E. V. Gorbar, V. P. Gusynin, V. A. Miransky and I. A. Shovkovy, Phys. Rev. B **66**, 045108 (2002).
[11] I. L. Aleiner, D. E. Kharzeev and A. M. Tsvelik, Phys. Rev. B **76**, 195415 (2007).
[12] J. E. Drut and D. T. Son, Phys. Rev. B **77**, 075115 (2008).
[13] O. Vafek and M. J. Case, Phys. Rev. B **77**, 033410 (2008).
[14] J. E. Drut and T. A. Lähde, Phys. Rev. Lett. **102**, 026802 (2009); Phys. Rev. B **79**, 241405(R) (2009).
[15] See also S. J. Hands and C. G. Strouthos, Phys. Rev. B **78**, 165423 (2008); W. Armour, S. Hands, C. Strouthos, Phys. Rev. B **81**, 125105 (2010).
[16] O. V. Gamayun, E. V. Gorbar and V. P. Gusynin, Phys. Rev. B **80**, 165429 (2009).
[17] J. Wang, H. A. Fertig and G. Murthy, Phys. Rev. Lett. **104**, 186401 (2010).
[18] J. González, Phys. Rev. B **82**, 155404 (2010).
[19] J. Wang, H. A. Fertig, G. Murthy and L. Brey, Phys. Rev. B **83**, 035404 (2011).
[20] O. V. Gamayun, E. V. Gorbar and V. P. Gusynin, Phys. Rev. B **81**, 075429 (2010).
[21] D. V. Khveshchenko, J. Phys.: Condens. Matter **21**, 075303 (2009).
[22] J. Sabio, F. Sols and F. Guinea, Phys. Rev. B **82**, 121413(R) (2010).
[23] D. J. Amit and V. Martín-Mayor, *Field Theory, the Renormalization Group, and Critical Phenomena*, Chaps. 6 and 8 (World Scientific, Singapore, 2005).
[24] J. González, F. Guinea and M. A. H. Vozmediano, Nucl. Phys. B **424**, 595 (1994).
[25] J. González, F. Guinea and M. A. H. Vozmediano, Phys. Rev. B **59**, R2474 (1999).
[26] We note that the vertex may depend on further many-body corrections to the screening of the interaction potential, though the most significant effect of Fermi velocity renormalization in the polarization, not considered here, can only lead to a reduction of the screening and therefore to lower values of the critical coupling for chiral symmetry breaking.
[27] P. Ramond, *Field Theory: A Modern Primer*, Chap. IV (Benjamin/Cummings, Reading, 1981).
[28] See also I. F. Herbut, V. Juričić and O. Vafek, Phys. Rev. B **80**, 075432 (2009); V. Juričić, I. F. Herbut and G. W. Semenoff, Phys. Rev. B **80**, 081405 (2009).
[29] D. C. Elias, R. V. Gorbachev, A. S. Mayorov, S. V. Morozov, A. A. Zhukov, P. Blake, L. A. Ponomarenko, I. V. Grigorieva, K. S. Novoselov, F. Guinea and A. K. Geim, Nature Phys. **7**, 701 (2011).
[30] O. Vafek and K. Yang, Phys. Rev. B **81**, 041401(R) (2010).
[31] F. Zhang, H. Min, M. Polini and A. H. MacDonald, Phys. Rev. B **81**, 041402(R) (2010).
[32] R. Nandkishore and L. Levitov, Phys. Rev. Lett. **104**, 156803 (2010).
[33] Y. Lemonik, I. L. Aleiner, C. Toke and V. I. Fal'ko, Phys. Rev. B **82**, 201408(R) (2010).